AIAA JOURNAL
Vol. 34, No. 1, January 1996

Application of the Finite Element Method to Acoustic Scattering Problems

J. A. Eaton* and B. A. Regan†
University College Galway, Galway, Ireland

For aircraft, scattering of engine and rotor noise from the fuselage and wings can considerably influence community and interior noise levels. Here the finite element method (FEM) is considered as a modeling technique because of its ability to solve for a broad range of governing equations and its potential efficiency advantages over the more commonly used boundary element method. With FEM, however, the data storage requirements become very demanding for three-dimensional problems involving realistic geometries and frequency ranges. To enable large FEM problems to be tackled using relatively modest computing facilities, the computational cost is addressed at several levels. The extent of the mesh is reduced using infinite elements; the data are manipulated using a sparse storage scheme; and an iterative complex solver in combination with a preconditioner is implemented. Validation of the code is illustrated by comparison with classical analytical solutions for plane wave scattering from a sphere. To demonstrate the potential of the technique, results are calculated for three-dimensional acoustic scattering off a fuselage geometry at useful frequencies.

Nomenclature

A	= distance from pole surface to inner face of infinite element
a	= characteristic length scale of problem
D_{ij}	= equivalent damping matrix
K_{ij}	= equivalent stiffness matrix
k	= wave number
M	= infinite element shape functions
M_{ij}	= equivalent mass matrix
N	= finite element shape function
n	= normal coordinate
P	= acoustic pressure
P_j	= pressure nodal values
R	= distance from pole surface
S	= element surface
V	= element volume; acoustic velocity
W	= finite element weighting function
ξ, η, ε	= local element coordinates
ρ	= fluid density
ω	= angular frequency

Subscripts

I	= incident
i, j	= matrix row/column identifiers
n	= normal component
S	= scattered
T	= total

I. Introduction

SCATTERING phenomena are known to considerably alter both interior and exterior noise fields of aircraft, where engine and propeller noise are scattered by the presence of fuselage, wing, and other surfaces. Although existing aeroacoustic prediction methods for aircraft engines, and especially for rotors, based on the equation of Ffowcs–Williams and Hawkings[1] are highly developed, they do not include scattering or refraction effects. These phenomena must be included if accurate acoustic predictions are to be made for aircraft. Classical, analytical scattering prediction techniques can only be applied to simple shapes such as spheres and plates and as such are of limited use when modeling realistic aircraft geometries in realistic flows. Semiempirical models are likewise limited by reliance on the availability of appropriate measurement sets. Numerical schemes offer the greatest potential for accurate predictions of scattering from complex aircraft shapes and have already been used for this purpose.[2,3] Both the finite element method (FEM) and the boundary element method (BEM) have been applied to these problems; in this paper we consider developments of the finite element approach.

The finite element technique has been found to be competitive in terms of computational effort with boundary element formulations for certain cases.[2–5] If a field solution is required of the boundary element method, then to find the pressure at any particular point, a separate integration over the complete surface of the radiating objects must be performed. This becomes computationally demanding for complex geometries and for high frequencies. In comparison, the FEM yields a continuous solution distribution over the entire domain. In comparing the two techniques, Burkhart et al.[2] found the BEM suitable for scattering problems involving simple configurations up to a ka value of approximately 3. Beyond this range, however, the method was too expensive for predicting scattering from a body with a complex geometry such as an aircraft, leading to the FEM as the preferred choice.

The use of infinite elements greatly improves the competitiveness of the FEM for exterior acoustic problems where a solution is required over an extensive far field.[4,5] The finite element solution extends over the entire infinite element region, so that results are calculated for the complete far field at little additional cost. If a solution over a range of frequencies is required, the FEM is even more favorable. This results because the finite element system matrix is independent of the wave number, whereas the boundary element matrix is not. The system matrix of the BEM must therefore be recalculated for each value of wave number. Moreover, unlike the BEM, the finite element method does not suffer from the well-documented nonuniqueness problem.

In addition to these efficiency advantages, the FEM can include a realistic flowfield model, whereas the BEM is inherently restricted in this respect. Flowfield effects are of considerable importance in aeroacoustic phenomena and a realistic flow model must be included if accurate predictions are to be made. The FEM promises a solution method for a very broad range of aeroacoustic equations. A comprehensive aeroacoustic flow model is feasible for axisymmetric problems, and for the three-dimensional case a compressible

Presented as Paper 93-4339 at the AIAA 15th Aeroacoustics Conference, Long Beach, CA, Oct. 25–27, 1993; received Jan. 26, 1994; revision received July 17, 1995; accepted for publication July 19, 1995.

*Director, Aerospace Research Unit. Senior Member AIAA.
†Doctoral Candidate, Department of Mechanical Engineering. Student Member AIAA.

potential flowfield with a boundary-layer approximation can be implemented economically. Acoustostructural coupling for interior noise calculations[6] may be modeled with the FEM, along with propagation in inhomogeneous media, such as cases involving thermal[7] or flow[8] gradients. In addition, detailed models of source mechanisms and of source distributions may be incorporated and solved for within the solution domain.

In general, the main drawback with the conventional FEM for these tasks is the generation and storage of vast amounts of data. To begin with, resolution of the shortest wavelength under consideration demands a fine mesh to be used for satisfactory results. This mesh density must be sustained in all directions over the entire domain and does not decrease away from the source. In addition, since the sound radiates to a three-dimensional domain of infinite extent, and because conventional far-field boundary conditions are only valid at a relatively large distance from the source, the domain is generally extensive. This results in a very large number of degrees of freedom. The conventional direct FE solution procedures[9] further exacerbate the data size problem as fill-in terms are generated during solution.

Several techniques are adopted in this paper to alleviate this data storage difficulty. The domain must be made finite by imposing a suitable boundary condition at a distant boundary. Infinite elements are used here instead of the more usual Sommerfeld radiation condition. This boundary condition allows a considerable reduction in domain size, because it is valid relatively near the radiating source. This is discussed in Sec. III.

Finite element solvers have traditionally employed direct solution methods. To solve realistic, three-dimensional problems of the type and size discussed here, such direct solvers require a prohibitively large amount of storage. Instead, we adopt an iterative solver based on the biconjugate gradient method to solve the finite element matrix, which is complex and nonsymmetric. In addition, our method is easily run out-of-core, so that the maximum problem size is not limited by the available computer storage, and solutions on low-cost workstations become tractable. A preconditioner that is based on an incomplete lower-upper (ILU) decomposition[10] is used to improve convergence rates.

The finite element matrix is very sparse for the three-dimensional problems in question. It is wasteful to either store or to operate on the zero values. To avoid this and to maximize efficiency, a sparse storage and manipulation scheme is devised. This method calculates, manipulates, and stores only the nonzero components of the equation set. This results in substantial savings, both in memory requirements and in computational effort.

The following sections outline the theory and techniques used in our FEM. The acoustic equations and their finite element formulation are presented in Sec. II. In Sec. III the infinite element representation of the far field is explained. The iterative solver, preconditioner, and sparse storage schemes are described and their advantages outlined in Sec. IV. Section V illustrates the validation of the code by comparing FEM predictions with classical analytical solutions for scattering from a sphere, and finally in Sec. VI a realistic application is demonstrated by calculating the sound field scattered off an aircraft geometry at useful frequencies.

II. Finite Element Representation of Problem

In the following analysis the finite element method is used to solve the Helmholtz equation,

$$\nabla^2 P + k^2 P = 0 \tag{1}$$

This frequency domain equation governs acoustic propagation in a three-dimensional space. Significant difficulties are not anticipated in extending this analysis to the three-dimensional perturbed potential flow equations. A Galerkin weighted residual scheme is used to form the required integral equation

$$\iiint_V (\nabla^2 P + k^2 P) W_i \, dV = 0 \tag{2}$$

The divergence theorem is applied to the Laplacian operator to reduce the equation to first order,

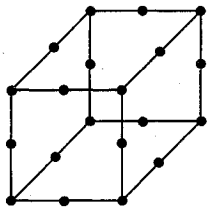

Fig. 1 Twenty-node serendipity element.

$$k^2 \iiint_V P W_i \, dV - \iiint_V (\nabla P \cdot \nabla W_i) \, dV + \iint_S W_i \left(\frac{\partial P}{\partial n} \right) dS = 0 \tag{3}$$

which reduces the interelement continuity requirements. This operation yields a surface integral term that can be used to apply the natural boundary condition. Across each element the pressure variable is discretized by representing it as a finite series of suitable polynomials N_j and unknown coefficients P_j:

$$P = \sum_{j=1}^{n} P_j N_j \tag{4}$$

As standard in the Galerkin procedure, these polynomials, or shape functions, are used as weighting functions:

$$k^2 \iiint_V N_i N_j \, dV P_j - \iiint_V (\nabla N_i \cdot \nabla N_j) \, dV P_j + \iint_S N_i \left(\frac{\partial P}{\partial n} \right) dS = 0 \tag{5}$$

We choose a 20-node brick element of the serendipity family to discretize the domain (Fig. 1). The shape functions of this element are second order.

Serendipity elements are computationally more efficient than their second-order Lagrangian equivalents[11]; the 27-node Lagrangian brick has 7 interior nodes. The rate of convergence of an element depends on the degree of the highest complete polynomial in the element trial function. The internal nodes generate extra, higher degree terms that do not contribute to completeness and thus render the Lagrangian element less efficient than the 20-node serendipity element.

A reduced integration scheme is used to evaluate integrals over the element. The error this introduces compensates, to some extent, for the stiffening effect of the finite element discretization and yields better results. The use of fewer integration points also results in a considerable reduction in computational requirements.

A standard FE pre- and postprocessor package[12] is used to generate the mesh, enabling complex geometries to be easily modeled. As is standard in finite element work, the shape functions of the standard parent element are used. An isoparametric mapping is used to map the parent element to the distorted element. As a rule of thumb, 5 quadratic elements (11 nodes)[13] per wavelength are used when generating a mesh. This is deemed necessary to ensure satisfactory accuracy.

III. Infinite Elements

A reflection-free radiation boundary condition is required at the specified exterior domain boundary. The Sommerfeld radiation condition,

$$\frac{\partial P}{\partial n} + ikP \to 0 \qquad \text{as} \qquad R \to \infty \tag{6}$$

is usually used for this purpose. As the distance from the radiating source becomes infinite, this expression is exactly valid. In a numerical model, this boundary condition is conveniently specified at a large, but finite, distance from the source. There is a conflicting desire, however, to place the outer boundary as close to the source

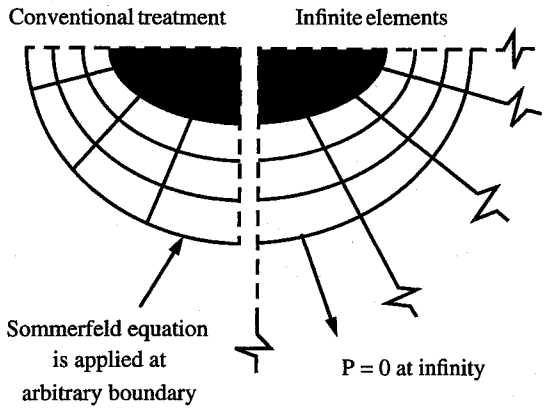

Fig. 2 Conventional and infinite element treatment of free radiation boundary condition.

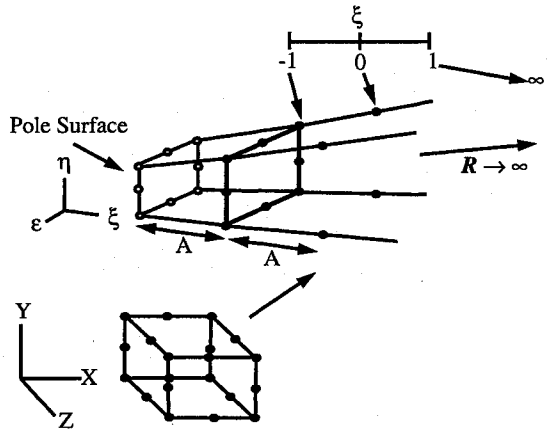

Fig. 3 Mapping of infinite elements.

as possible so that the extent of the mesh, and hence the computational problem size, is kept to a reasonable minimum. This conflict compromises the validity of the Sommerfeld boundary condition. In this work an alternative model of the far field behavior is used. Instead of applying the Sommerfeld radiation condition to the far field boundary, the outer domain is modeled using infinite elements. This enables the conventional mesh to be restricted to the region near the radiating source, thus greatly reducing the required mesh extent. An added advantage of this approach is that the entire acoustic far field can quickly be calculated from the infinite element solution.

Infinite elements were originally developed by Bettess[14] and Bettess and Zienkiewicz[15] and have been used extensively in surface wave analysis. Similar techniques have since been applied to exterior aeroacoustic problems.[7,8,13,16,17] These elements are used in problems of infinite or semi-infinite domains. The conventional finite elements are coupled to elements of the type sketched in Fig. 2, which model the domain stretching towards infinity. If the nature of the far-field solution is known, it can be embodied within the shape functions of the infinite element. In a stationary medium, the acoustic field is propagating with exponential character $\exp(-ikR)$ and decaying by a factor of $1/R$, where R is the distance from the pole surface as indicated in Fig. 3. Thus,

$$P \propto (e^{-ikR})/R \tag{7}$$

Surfaces of constant R are surfaces of constant phase and the inner face of the infinite element is placed on this surface. In these elements the shape functions are modified to embody, within the element, complex exponential propagation. The modified shape functions are thus

$$M_j = N_j \exp\{-ik[R(\xi, \eta, \varepsilon) - A(\eta, \varepsilon)]\} P_j \tag{8}$$

where N_j are the conventional shape functions, and $A(\eta, \varepsilon)$ is the distance from the pole surface to the inner face of the infinite element as indicated in Fig. 3.

To ensure compatibility with the conventional elements the shape functions are required to be continuous at the common boundary of the finite and infinite elements. The absolute value of the shape function at $\xi = -1$ must be unity and its phase must be zero to achieve this. Note that at the finite face of the infinite element the modified shape function reduces to N_j, so that this criterion is ensured.

The infinite element uses a mapping function to implement the $1/R$ decay behavior. In the direction of propagation, the mapping of the element is given by

$$R(\xi, \eta, \varepsilon) = 2\frac{A(\eta, \varepsilon)}{(1 - \xi)} \tag{9}$$

where the local coordinate ξ lies in the direction of propagation. Therefore, the inverse mapping is given by

$$\xi = 1 - (2A/R) \tag{10}$$

The unknown pressure is approximated by a polynomial variation in local coordinates,

$$P = \alpha_0 + \alpha_1 \xi + \alpha_2 \xi^2 + \cdots \tag{11}$$

which, using Eq. (10), maps to

$$P = \beta_0 + (\beta_1/R) + \left(\beta_2/R^2\right) + \cdots \tag{12}$$

where β_0 is zero because P decays to zero when R becomes infinite. More detail on the mapping function is given in Ref. 18.

The choice of weighting function is very important. At first, infinite elements used the conventional shape functions for this purpose, which resulted in integral expressions that involved exponential terms. This necessitates the use of Gauss–Laguerre integration rules, instead of the usual Gauss–Lagrange integration schemes, which are not suitable for exponential expressions. Astley and Eversman[16] and Astley[17] overcame this problem by using the complex conjugates of the shape functions as weighting functions in their wave envelope elements, which causes the exponential terms to cancel out in the integral expressions. These wave envelope elements are large, but finite, elements. Several layers of these elements[7,8] are used to extend the mesh to a distant, but again finite, boundary where the Sommerfeld condition is applied. If it is necessary to keep the number of elements to a minimum, however, elements of infinite extent are preferable.

The wave envelope type of weighting function has been adapted for elements of infinite extent by Astley and Coyette.[4] Their new weighting function is

$$W_i(\xi, \eta, \varepsilon) = (A/R)^2 N_i(\xi, \eta, \varepsilon) e^{ik(R-A)} \tag{13}$$

For these infinite elements, Eq. (5) now becomes

$$k^2 \iiint_V W_i M_j \, dV P_j - \iiint_V (\nabla W_i \cdot \nabla M_j) \, dV P_j + \iint_S W_i \left(\frac{\partial P}{\partial n}\right) dS = 0 \tag{14}$$

These volume integral expressions are expanded into equivalent mass, stiffness, and damping matrices:

$$-k^2[M_{ij}] = -k^2[(A/R)N_i N_j\{1 - [\nabla(R - A) \cdot \nabla(R - A)]\}] \tag{15}$$

$$[K_{ij}] = [(A/R)\nabla N_i \cdot \nabla N_j + N_i[\nabla(A/R) \cdot \nabla N_j]] \tag{16}$$

$$ik[D_{ij}] = ik[(A/R)N_i \nabla(R - A) \cdot \nabla N_j - N_j[(A/R)\nabla N_i + N_i \nabla(A/R)] \cdot \nabla(R - A)] \tag{17}$$

These matrices are complex and unsymmetric but contain no exponential terms. We also note that they are not dependent on the wave number k. Here is one considerable advantage of this formulation; for solutions over a range of frequencies the matrices need only be evaluated and assembled once.

IV. Iterative Solver and Sparse Storage Scheme

A large number of degrees of freedom are required for external aeroacoustic finite element models. Not only is the domain itself extensive but also a fine mesh is dictated. The global matrices generated from these meshes cannot be treated efficiently using conventional FEM. Direct solution methods have traditionally been employed for FEM solutions. In general, such methods do not take full advantage of the sparseness of the matrix and demand a large data storage capacity because the number of stored terms is greatly increased during solution as fill-in terms are generated. The alternative is to use an iterative solver that fully exploits this sparseness. Such a scheme is utilized in this work.

It is found necessary to employ a preconditioner to ensure satisfactory convergence rates. A scheme based on an ILU decomposition[10] is implemented. The preconditioner is adjustable so that the convergence performance can be balanced against the computational cost of the preconditioner. Two control parameters are used—the first drops terms that are below a given tolerance and the second limits the number of terms allowed in a row. Thus both the computational time and memory demands of the preconditioner can be effectively controlled.

The finite element matrices discussed in this case are very sparse. Recall that 20-node elements are used, with 1 degree of freedom per node—pressure. Thus, the maximum number of nodes that form terms with a particular node is 81, so that the maximum number of nonzero terms that may occur in any row of the matrix is also 81 (this applies to a corner node that is attached to 8 other elements). Midside nodes, or nodes connected to fewer elements, form fewer terms. This figure of 81 does not increase as the number of nodes in the mesh increases, so that the matrix becomes more sparse for larger problems. Accordingly, for the class of problems discussed in this paper, which are large and three dimensional and have only one degree of freedom per node, the matrices are especially sparse.

When direct solution methods are used, the number of nonzero terms on each row increases rapidly as elimination proceeds. This imposes an effective limit on the size of problems that these methods can handle, as data storage requirements become too demanding on the computer system. In this study we employ a scheme that only stores and operates on nonzero terms. This results in profound savings in computational effort and in storage requirements, the storage requirement being directly proportional to the number of solution variables. The nonzero terms of the two-dimensional matrix are stored row by row in a one-dimensional array. Two tag arrays are used to track the position of the one-dimensional array terms in the original two-dimensional matrix. The first records the position, in the one-dimensional array, of each term that starts a new row. The second records the columnar position of each term in the array. Using this procedure, the iterative solver can efficiently track and access all terms in the matrix.

The iterative solver used here is based on the biconjugate gradient algorithm, a version of the conjugate gradient method.[19] The algorithm is applied in conjunction with the sparse storage scheme and ILU preconditioner just discussed.

V. Validation

Preliminary validation of our FEM, as applied to the scattering problem, is illustrated by comparing three-dimensional field predictions with analytical solutions for the case of scattering of an acoustic plane wave by a rigid sphere. The analytical solution for this problem is given in Ref. 20. We divide the total pressure into incident and scattered components:

$$P_T = P_I + P_S \tag{18}$$

Both pressure components satisfy Eq. (1). The boundary condition on the surface of the rigid sphere is

$$\frac{\partial P_S}{\partial n} = -\frac{\partial P_I}{\partial n} \tag{19}$$

which can be written as

$$\frac{\partial P_S}{\partial n} = -i\rho\omega V_n \tag{20}$$

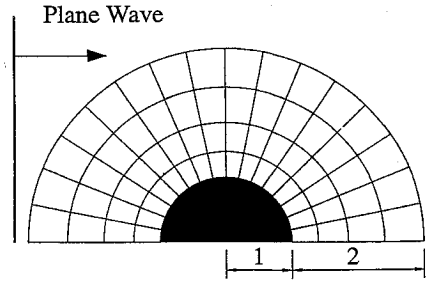

Fig. 4 Near-field finite element mesh for sphere, sized for five elements/wavelength and $ka = 2.0$.

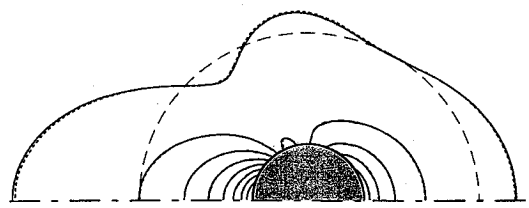

Fig. 5 Predicted (- - -) and analytical (—) acoustic pressure contours in the near field for $ka = 2.0$.

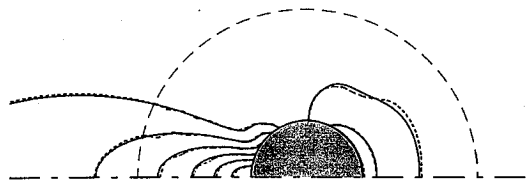

Fig. 6 Suboptimal mesh: predicted (- - -) and analytical (—) acoustic pressure contours for $ka = 5.0$.

where the normal velocity magnitude V_n is given by

$$V_n = -\frac{1}{i\rho\omega}\frac{\partial P_I}{\partial n} \tag{21}$$

The solution is symmetric about an axis parallel to the direction of propagation of the plane wave, so that only one-quarter of the sphere needs to be modeled. The natural boundary condition for symmetry is

$$\frac{\partial P}{\partial n} = 0 \tag{22}$$

The near field is meshed using 224 elements arranged in 4 rows, and 56 infinite elements are used for the far field (Fig. 4). These problems required approximately 40 iterations, where convergence was considered complete when the normalized residual had fallen to double precision zero. The normalized residual is defined as the L_2 norm of the nodal residuals, normalized to the L_2 norm of the forcing vector.

Results are presented in Figs. 5 and 6 for two values of ka. Taking five elements per wavelength, the mesh is suitably sized for $ka = 2$. Even up to the value of $ka = 5$, however, where the mesh is suboptimal, there is close agreement between the analytical solution and the numerical prediction.

VI. Application

The combination of techniques described in this paper enables the solution of aircraft noise fields at useful frequencies using workstation-type computers. At lower frequencies entire aircraft can be enclosed in the solution domain. To illustrate the potential of the method, the pressure field around a representative aircraft fuselage geometry due to a single source has been calculated.

The fuselage is a filleted box section that is tapered fore and aft. Figure 7 illustrates the fuselage geometry and the location of the source. The source is above the surface and off axis so as to produce a nonsymmetric acoustic field.

The model consists of 60,000 nodes and 13,500 quadratic hexahedral elements, which yields a mesh of sufficient density to solve for

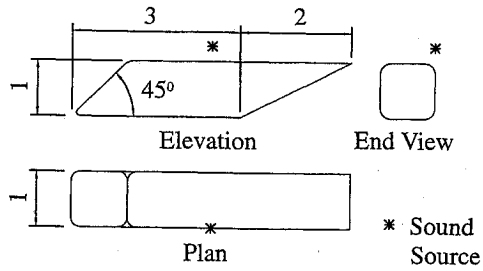

Fig. 7 Fuselage geometry and source location.

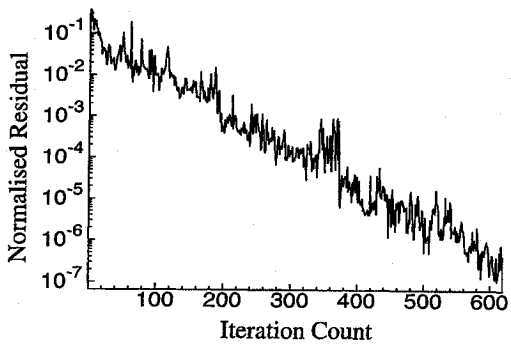

Fig. 8 Convergence history for 60,000 node case.

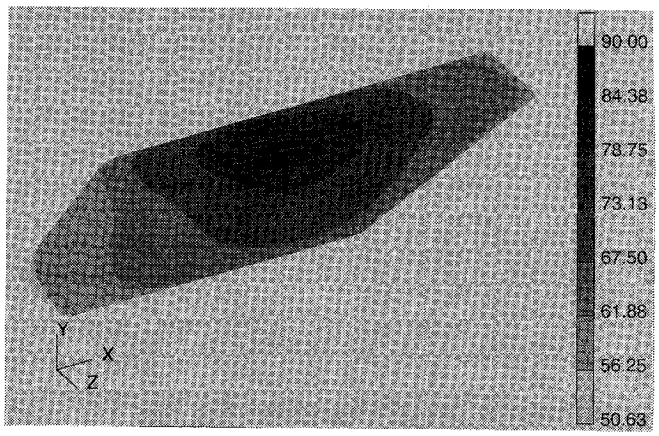

Fig. 9 Fuselage surface pressure (dB).

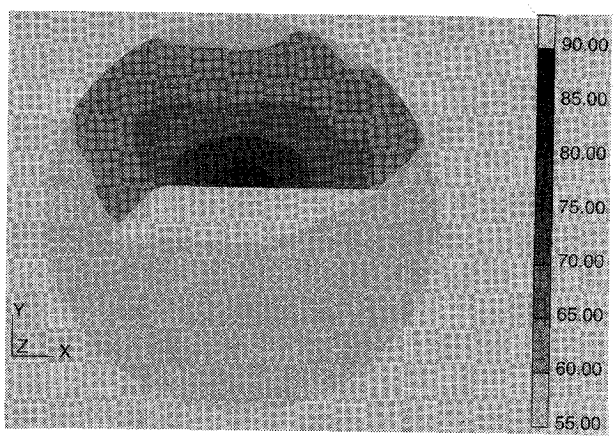

Fig. 10 Pressure field on fuselage center plane.

a *ka* value of 20. Although this is a problem of considerable size, the memory requirement for the complex finite element matrices is only around 50 Mbytes, where all numbers are of double precision accuracy. This size problem can be comfortably run in-core on modern workstations. Convergence to a normalized residual of 10^{-8} required approximately 600 iterations (Fig. 8) for this problem. We note that in this case the preconditioner was not adjusted for optimal convergence performance.

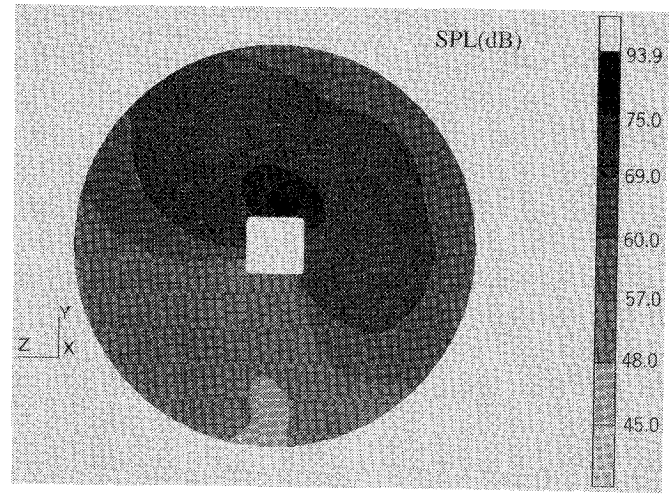

Fig. 11 Pressure field on midlength cross-sectional plane.

The sound pressure level fields due to the source at a *ka* value of 18 are presented in Figs. 9–11. Figure 9 shows the fuselage surface pressure distribution as would be required for estimating cabin noise. The sectional views (Figs. 10 and 11) indicate the significant shielding effect of the fuselage. This example demonstrates the potential and usefulness of the approach described in this paper.

VII. Conclusions

The three-dimensional Helmholtz equation has been formulated for numerical solution using an innovative development of the FEM. Infinite elements allow accurate modeling of radiation to the far field with minimal computational effort. The implementation of a preconditioned iterative solver and of a sparse storage scheme, which combine to make efficient use of storage space, allows problems of realistic size to be solved using relatively modest computing facilities. The method displays close agreement with the analytical solution for plane wave scattering by a rigid sphere. To demonstrate the applicability of the method it is used to solve for the acoustic field of a realistic aircraft fuselage geometry.

Acknowledgments

We appreciate the assistance of the following colleagues at the Aerospace Research Unit: Nathan Quinlan for coding the analytical solution and Joseph Kilcullen for preparing the fuselage model.

References

[1]Ffowcs-Williams, J. E., and Hawkings, D. L., "Sound Generation by Turbulence and Surfaces in Arbitrary Motion," *Philosophical Transactions of the Royal Society, Series A: Mathematical and Physical Sciences*, Vol. A264, 1969, pp. 321–342.

[2]Burkhart, R. H., SenGupta, G., Johnson, F. T., Bussoletti, J. E., Young, D. P., Melvin, R. G., Samant, S. S., and Bieterman, M. B., "Numerical Prediction of Scattering of Acoustic Waves by an Aircraft," 2nd IMACS Symposium on Computational Acoustics, Princeton, NJ, March 1989.

[3]SenGupta, G., Burkhart, R. H., Bussoletti, J. E., Johnson, F. T., Melvin, R. G., Young, D. P., and Bieterman, M. B., "Application of Computational Methods in Aeroacoustics," AIAA Paper 90-3917, Oct. 1990.

[4]Astley, R. J., and Coyette, J. P., "Mapped Wave Envelope Elements of Infinite Extent: Applications to Acousto-Structural Scattering," International Conference on Recent Advances in Structural Dynamics, Southampton, England, UK, July 1991.

[5]Burnett, D. S., "Structural Acoustic Modelling Using a New High Accuracy Acoustic Infinite Element," 7th World Congress on FEM, Monaco, Nov. 1993.

[6]Coyette, J. P., "Validation of a New Wave Envelope Formulation for Handling Exterior Acoustic and Elasto-Acoustic Problems in the Frequency Domain," DGLR/AIAA Paper 92-02-073, May 1992.

[7]Astley, R. J., and Eversman, W., "Wave Envelope Elements for Acoustical Radiation in Inhomogeneous Media," *Computers and Structures*, Vol. 30, No. 4, 1988, pp. 801–810.

[8]Parrett, A. V., and Eversman, W., "Wave Envelope and Finite Element Approximations for Turbofan Noise Radiation in Flight," *AIAA Journal*, Vol. 24, No. 5, 1986, pp. 753–759.

[9]Carey, G. F., and Oden, T. J., *Finite Elements: Vol. III—Computational Aspects*, Prentice–Hall, Englewood Cliffs, NJ, 1984, Chap. 3.

[10]Saad, Y., "Preconditioning Techniques for Nonsymmetric and Indefinite Linear Systems," *Journal of Computational and Applied Mathematics*, Vol. 24, 1988, pp. 89–105.

[11]Burnett, D. S., *Finite Element Analysis*, AT&T Bell Lab., Whippany, NJ, 1987.

[12]Anon., "P3/Patran User Manual," PDA Engineering, Costa Mesa, CA, April 1993.

[13]Eversman, W., "Radiated Noise of Ducted Fans," DGLR/AIAA Paper 92-02-139, May 1992.

[14]Bettess, P., "Infinite Elements," *International Journal for Numerical Methods in Engineering*, Vol. 11, 1977, pp. 53–64.

[15]Bettess, P., and Zienkiewicz, O. C., "Diffraction and Refraction of Surface Waves Using Finite and Infinite Elements," *International Journal for Numerical Methods in Engineering*, Vol. 11, 1977, pp. 1271–1290.

[16]Astley, R. J., and Eversman, W., "A Note on the Utility of a Wave Envelope Approach in Finite Element Duct Transmission Studies," *Journal of Sound and Vibration*, Vol. 76, No. 4, 1981, pp. 595–601.

[17]Astley, R. J., "Wave Envelope and Infinite Elements for Acoustic Radiation," *International Journal for Numerical Methods in Fluids*, Vol. 3, 1983, pp. 507–526.

[18]Zienkiewicz, O. C., and Taylor, R. L., *The Finite Element Method*, Vol. 1, 4th ed., McGraw–Hill, London, 1989, pp. 183–189.

[19]Golub, G. H., and Van Loan, C. F., *Matrix Computations*, 2nd ed., John Hopkins Univ. Press, Baltimore, MD, 1989.

[20]Skudrzyk, E., *The Foundations of Acoustics*, Springer–Verlag, New York, 1971, pp. 408–413.